ARPN Journal of Engineering and Applied Sciences

ANALYSIS OF SOME ENGINEERING PARAMETERS RELEVANT TO THE PERFORMANCE AND RELIABILITY OF HOLLOW FIBER SPINNING SYSTEM

Shadia R. Tewfik[1], Abdel Ghani M. G.Abulnour[1], Hayam F. Shaalan[1], Mohamed I. El-Anwar[2], Sahar S. Ali[1], Kamal A. Abed[2], Mervat A. Badr[2] and Mohamed H. Sorour[1]
[1]Department of Chemical Engineering and Pilot Plant, National Research Centre, Engineering Research Division, ElBohous St. Dokki, Giza, Egypt
[2]Department of Mechanical Engineering, National Research Centre, Engineering Research Division, ElBohous St. Dokki, Giza, Egypt
E-Mail: shadiatewfik@yahoo.com

ABSTRACT

Hollow Fiber (HF) membranes manifest wide applications on numerous environmental and industrial fields. The remarkable characteristics of high surface to volume ratio and compaction motivated the rapid advancement of HF technology and engineering. The spinning system is subject to numerous parameters and variables that critically influence the characteristics and performance of the produced HF. This paper outlines theendeavors to develop cellulose acetate (CA) HF membrane prepared by dry-wet spinning under varying dope, rheological settings and conditions in addition to spinning nozzle types and dimensions. Computational fluid dynamics (CFD) analysis has been used to simulate the travel of the polymer inside the spinneret. Characterization results using scanning electron microscope (SEM), atomic force microscopy (AFM) and mechanical properties are outlined. Furthermore, the effect of the fore-mentioned parameters on water flux is addressed. Moreover, the fabrication of polysulfone/polyethersulfone (PS/PES) HF has been investigated with the aim of comparing structure, morphology and properties with CA fibers. The paper is concluded with recommendations pertinent to fabrication of CA and PS/PES hollow fiber membranes.

Keywords: hollow fiber, cellulose acetate, polyether sulfone, spinning, characterization, performance.

INTRODUCTION

Membrane processes and particularly hollow fiber membranes (HF) Treatment technology for water recycling encompasses a vast number of options. Membrane processes are regarded as key elements of advanced wastewater reclamation and reuse schemes and are included in a number of prominent schemes world-wide, e.g. for artificial groundwater recharge, indirect potable reuse as well as for industrial process water production Treatment technology for water recycling encompasses a vast number of options. Membrane processes are regarded as key elements of advanced wastewater reclamation and reuse schemes and are included in a number of prominent schemes world-wide, e.g. for artificial groundwater recharge, indirect potable reuse as well as for industrial process water production Treatment technology for water recycling encompasses a vast number of options. Membrane processes are regarded as key elements of advanced wastewater reclamation and reuse schemes and are included in a number of prominent schemes world-wide, e.g. for artificial groundwater recharge, indirect potable reuse as well as for industrial process water production Treatment technology for water recycling encompasses a vast number of options. Membrane processes are regarded as key elements of advanced wastewater reclamation and reuse schemes and are included in a number of prominent schemes world-wide, e.g. for artificial groundwater recharge, indirect potable reuse as well as for industrial process water production Treatment technology for water recycling encompasses a vast number of options. Membrane processes are regarded as key elements of advanced wastewater reclamation and reuse schemes and are included in a number of prominent schemes world-wide, e.g. for artificial groundwater recharge, indirect potable reuse as well as for industrial process water produ Treatment technology for water recycling encompasses a vast number of options. Membrane processes are regarded as key elements of advanced wastewater reclamation and reuse schemes and are included in a number of prominent schemes world-wide, e.g. for artificial groundwater recharge, indirect potable reuse as well as for industrial process water production Treatment technology for water recycling encompasses a vast number of options. Membrane processes are regarded as key elements of advanced wastewater reclamation and reuse schemes and are included in a number of prominent schemes world-wide, e.g. for artificial groundwater recharge, indirect potable reuse as well as for industrial process water production Treatment technology for water recycling encompasses a vast number of options. Membrane processes are regarded as key elements of advanced wastewater reclamation and reuse schemes and are included in a number of prominent schemes world-wide, e.g. for artificial groundwater recharge, indirect potable reuse as well as for industrial process water production Treatment technology for water recycling encompasses a vast number of options. Membrane processes are regarded as key elements of advanced wastewater reclamation and reuse schemes and are included in a number of prominent schemes world-wide, e.g. for artificial groundwater recharge, indirect potable reuse as well as for industrial process water production Treatment technology for water recycling encompasses a vast number of options.

Membrane processes are regarded as key elements of advanced wastewater reclamation and reuse schemes and are included in a number of prominent schemes world-wide, e.g. for artificial groundwater recharge, indirect potable reuse as well as for industrial process water production Treatment technology for water recycling encompasses a vast number of options. Membrane processes are regarded as key elements of advanced wastewater reclamation and reuse schemes and are included in a number of prominent schemes world-wide, e.g. for artificial groundwater recharge, indirect potable reuse as well as for industrial process water production Treatment technology for water recycling encompasses a vast number of options. Membrane processes are regarded as key elements of advanced wastewater reclamation and reuse schemes and are included in a number of prominent schemes world-wide, e.g. for artificial groundwater recharge, indirect potable reuse as well as for industrial process water production HFHHF which have specific features including high surface area to volume ratio, large porosity, good mechanical properties and good water permeability, are gaining wide attraction for water filtration applications including microfiltration, nanofiltration, reverse osmosis, gas separation , forward osmosis and pressure retarded osmosis [Baker (2004),Orofino *et al.* (1077), Nunes and Peinemann (2006)].

HF membranes are most commonly prepared by the dry - wet spinning process. The ideal spinning process would produce fibers of desired uniform size and morphology [Yang (2007)]. Modeling and numerical simulation of extrusion of polymers have been discussed by several authors [Antonietti *et al*. (2011), Tung (2012), Zhang (2013)]. Computational Fluid Dynamics (CFD) for the numerical simulation of the polymer and/or the bore fluid flow through the spinnerets has been adopted to ensure proper spinneret design and predict HF morphology [Cao *et al* (2004)].

The dry - wet spinning process involves numerous spinning parameters such as dope and bore compositions, flow rates, temperatures, take-up speed,…etc., making it extremely tedious to reproduce HF with a specified morphology and separation performance. Accordingly, it is vital to elucidate the effects of these parameters for optimizing membrane morphology and performance [Aptel *et al*. (1985), Chou *et al*. (2005), (2007), Chung *et al*. (1999),), Ehsan & Toraj (2009) Feng *et al*. (2013), Hao *et al*. (1996), Idris *et al.* (2002), Khayet (2003), Miyano *et al*. (1993), Ren *et al* (2008), Qin *et al*. (1999) (2003), (2005a,b)]. Higher dope flow rate leads to the formation of a hollow fiber with inner porous surface and dense selective layer on outer side which shows reduced water permeability but improved separation and Young's Modulus [Qin *et al*. (1999)]. Air-gap distance plays a very important role on the cross-section area of nascent fibers. Both the inner and outer diameters (Di and Do) of dry wet-spun fibers decrease with increase in air gap distance [Khayet (2003), Chung *et al.* (1999)]. An important controlling factor in HF preparation is the additives such as polyvinyl pyrrolidone (PVP) and polyethylene glycol (PEG) which are added to the dope solution to increase permeability. However, the addition of PVP or PEG with high molecular mass results in a low flux membrane as a result of swelling of the residual PVP or PEGat the surface of pore walls when water passes through the membrane pores [Chou *et al*. (2007), Ehsan & Toraj (2009), Miyano *et al.* (1993), Qin *et al*. (2003), (2005a,b)].

In addition to CA, polymers such as polysulfone (PSF), polyethersulfone (PES), polyacrylonitrile (PAN), polyvinyl alcohol (PVC) and polyvinylidene fluoride (PVDF) hollow fiber membranes are fabricated for various industrial and /or medical applications. However, most membranes of these materials are commonly obtained by thermally induced phase separation (TIPS) and non-solvent induced phase separation (NIPS) methods [Chen *et al.* (2005), Feng *et al.* (2013), Ren & Wang (2008)].

Shear rate is considered one of the most important parameters which affect the membrane morphology, mechanical properties and the performances of hollow fibers [Chung *et al* (2000)]. Many of the researchers analyzed thesystem consisting of fabricating the HF membrane through dry/wet inversion process using cellulose acetate as base polymer [Idris *et al*. (2002), (2003), Shieh & Chung (1998)]. The membrane rejection rate increases with the increase in shear rate. However authors concluded that there is an optimum shear rate for optimized membrane morphology [Idris *et al.* (2002), Shieh & Chung (1998)].

The effect of dope preparation and spinning parameters are manifested by membrane surface morphology (SEM and AFM) [Stamatialis *et al.* (1999)].For example, dense structure was obtained as depicted by SEM images, when coagulation bath was only composed of water. AFM images have revealed that both the nodular structure size and the roughness of the membrane outer surface were affected by the air gap distance, coagulation bath temperature and composition. Furthermore, the membrane preparation method (TIPS or NIPS) has profound effect on membrane surface roughness [Chou & Yang, (2005), Chung *et al*. (2002), Kim *et al*. (1999) Qin *et al.* (2003), Wienk *et al.* (1994), Xu & Qusay (2004), Zhang *et al*. (2002)].

This paper addresses, theoretical and numerical analysis relevant to design and validation of custom made spinneret for hollow fiber fabrication. Experimental investigations for HF preparation of CA based dopes on rheology of the spinning dopes are presented. Characteristics and performance of selected samples are analyzed and correlated to composition and spinning parameters. Results of some HF CA membranes and HF PES membranes are compared. Analysis of results provides indicators for HF fabrication with preferred morphology.

EXPERIMENTAL

Materials and methods

Materials

Cellulose acetate (CA) (acetyl content 39.3 wt%) and Cellulose triactate CTA 43-49 wt. % acetyl have been supplied from Sigma-Aldrich. (PVP) of different molecular weights (30°K, 40K, 90°K and 360°K) supplied from Sigma-Aldrich and Applichem has been used as the pore formers. Lithium chloride (LiCl) (MW= 42.30) has been supplied from Alpha Chemika. Polyethylene glycol (PEG) (400) has been purchased from Sigma Aldrich. Solvents, N-methyl-2- pyrrolidone (NMP) and N, N-dimethylacetamide (DMAc) have been supplied from Carl-Roth and Merck. Polysulfone and Polyethersulfonehave been purchased from BASF (Ultrason® S6010 and E6020P, respectively). Diethyl phthalate used as a plasticizer has been supplied from Carlo Erba Reagents. Acetone and ethanol have been provided as laboratory grade solvents. All chemicals have been used as received. RO water has been used for coagulation and washing.

Spinning systems

Two HF spinning systems have been employed. System (1) has been provided by FilaTech GmbH while System (2) has been customized specifically for spin block design and dimensions. The spinning systems essentially comprise feed tanks for the dope and bore fluids, spin block supported on a holder with adjustable air gap, coagulation and washing baths in addition to a winder. Dope and bore fluids are fed to the spin block using pressurized nitrogen, while a pump (Oerlikon Barmag) is used for feeding the dopein System (1) which is additionally provided by a dryer. The general scheme of the spinning systems is represented in Figure-1. Numerous spinnerets have been designed and fabricated as typically presented in Figure-2.

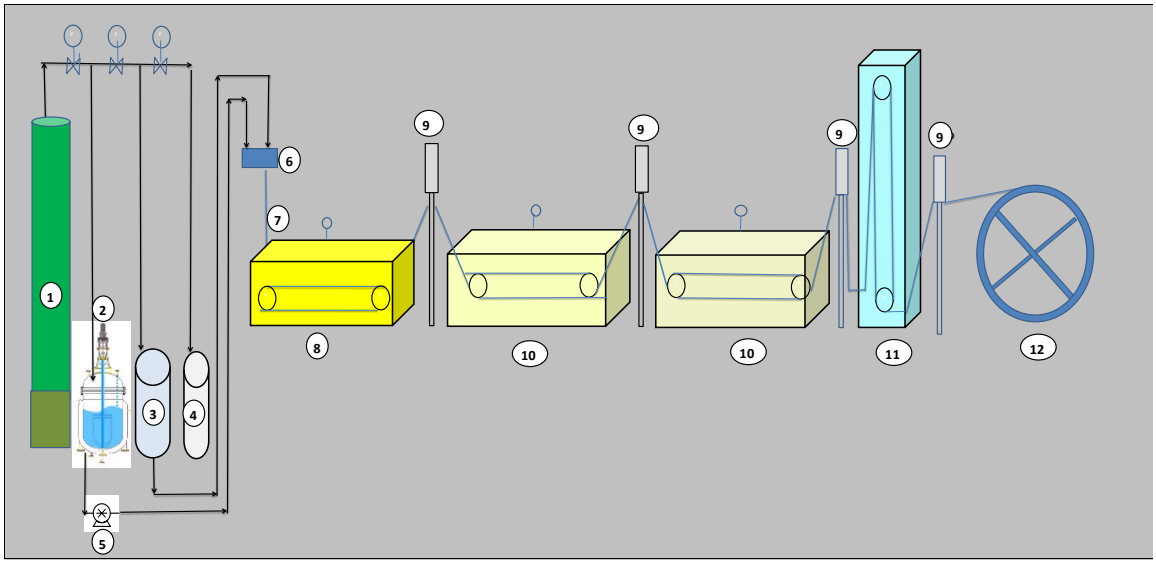

Figure-1. Schematic diagram for the hollow fiber membranes spinning system.
1: Nitrogen cylinder, 2: stirred tank reactor, 3: bore fluid vessel, 4: flushing solvent tank, 5: dope pump, 6: spin block, 7: air gap, 8: coagulation bath, 9: take-up roll unit, 10: wasing tank, 11: dryer, 12: reel winder.

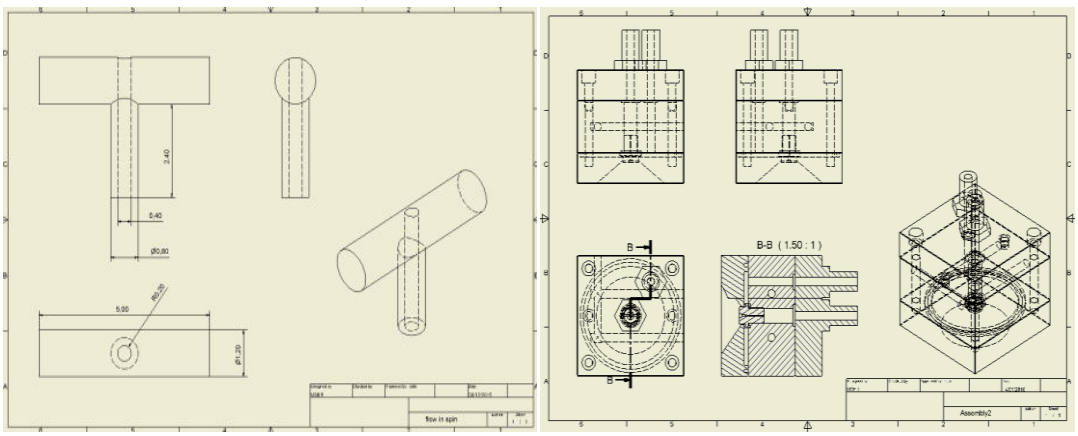

(a) (b)

Figure-2. (a) Spinneret design with internal needle, and (b) spin block for single spinneret.

Polymer blends

Various groups of polymer solutions have been prepared and fabricated to investigate the effect of composition and operating parameters on the characteristics and performance of the prepared fibers. These include essentially cellulose acetate with or without blends or additives. Other polymers comprise PS and or PES. Additives comprise PVP, PEG, or plasticizer (Pl). Solvents used have been mainly NMP and DMAc while, ethanol and acetone have been used as non-solvent in some samples. Table-1 depicts the composition, viscosities of typical coded samples which have been prepared using systems (1) or (2) while Table-2 compiles typical operating conditions.

Table-1. Composition and viscosity of the investigated dopes.

Sample code	Spinneret type	Polymers (%)	Additives (%)	Solvent (%)	Non-solvent (%)	Viscosity (Cp)
CA 1	Custom	CA -22		NMP-78		10500
CA 2		CA-19	PVP-3	NMP-78		5400
CA 3		CA-19	PEG-3	NMP-78		10700
CA 4		CA/PS- 22.5/4	PEG/PL/LICL-2/5/0.7	NMP-66.5	ET-1	35000
CA 5		CA/CTA-7.5/7.5	PEG-2	NMP-83		60500
CA 6		CA/CTA-11.5/5	PEG/PL-3.4/3.4	NMP-76		27500
CA 7	Procured	CA/PS-22/4	PVP/PEG-5/5	NMP-54	AC-10	19600
CA 8		CA/PES-20/3	PVP/PEG/PL-3/1/4	NMP-68	ET-1	27850
P9		PES-20	PVP/LiCl-7/0.5	NMP/DMAc-69/3.5		12500

Table-2. Operating conditions of the investigated dopes.

Investigated parameter	Value
Dope flow rate (system 1)	2.8-5 bar
Dope flow rate (system 2)	3.0-3.7 ml/min
Bore flow rate (system 1)	0.2-2.5 bar
Bore flow rate (system 2)	2-2.22 ml/min
Spin block temperature	30-50oC
Air gap length (G)	5-30 cm
Coagulation bath temperature	24-28^{o}C
Washing bath temperature	24-28^{o}C
Drying temperature	25-40^{o}C
Post treatment	Heating at 80oC for 10 mins

Characterization and measurements

Rheological properties

Rheological properties have been investigated for selected samples using Anton Paar Rheometer MCR-301. The measurements have been carried out using 10 cm plate-plate system at 25oC ± 0.2 for shear rate ranging from 10 to 1500 s -1. For all prepared samples, the dope viscosity has been determined using Brookfield Viscometer Model DV-E. Selected CA dopes (CA1-CA3) in Table-1 have been subjected to Rheological investigations.

Morphological surface analysis

The prepared HF membrane is examined by Scanning electron microscope (SEM model JEOL 5410 operating at 10-30 kV) to observe the microstructure. The prepared hollow fiber is first dried and fractured in liquid nitrogen, and then gold sputtering is applied to create a conductive layer. HFMs fabricated have been subjected to SEM studies. Details of cross section, fiber dimensions have been elucidated.

Membrane surface roughness using atomic force microscope (AFM)

Surface roughness has been measured for selected samples by TT-AFM workshop model with sample sizes up to 1"×1"×1/4", equipped with a video optical microscope with zoom up to 400X and 1.5 micron resolution. A 1 cm long fiber sample was fixed using a double face tape on the magnetic plate of the AFM apparatus. Vibrating scan mode was used for testing with scan area of 10µm×10µm. Roughness parameters have been calculated using "Gwyddion" software. Five fibers from each sample have been investigated for average roughness (Ra) and root mean square roughness (Rms).

Mechanical properties

Mechanical properties have been determined for representative samples using Tensile Testing Machine (Tinius Olsen model H5kS). Testing has been undertaken at 50 mm/min speed and grip separation of 100 mm. Tensile stress, elongation at break and fiber's modulus

have been measured. Stress - strain data have been characterized for typical samples.

Pure Water Permeability (PWP)

Pure water permeability tests have been conducted for selected samples on RO Permeability Test System provided by PHILOS Co., Ltd. The system comprises high pressure HF test cell, high pressure pump, feed & permeate tanks in addition to pressure gauge and flow meters.

Water performance analysis has been limited to CA HF samples (CA 4 and CA 8) and compared with PES sample (P9).

Spinneret design validation

Computational fluid dynamics (CFD) package has been used to confirm stability of velocity within the annular cavity of the spinneret.A spin block with a single spinneret has been designed and constructed within the scope of this work. Figure-2 shows the spinneret design with internal needle and its assembly in a single spinneret spin block in addition to the cut sections.

Computational fluid dynamics (CFD) analysis has been used to simulate the travel of the polymer inside the spinneret. As bore fluid and polymer do not mix inside the spinneret, the CFD analysis of the two fluids can be performed separately. The bore fluid is Reverse Osmosis (RO) water which passes directly through the tube in orifice of diameter ranging from 0.3 - 0.6mm, while the dope passes from its pool around the spinneret via a horizontal hole to be redirected downwards around the bore fluid tube and exit the spinneret coaxially. The CFD governing equations which have been considered for the polymer flow include;

1- Continuity Equation:

$$\frac{\partial U}{\partial x}+\frac{\partial V}{\partial y}+\frac{\partial W}{\partial z}=0 \quad \ldots (1)$$

2- Navier Stokes Equation:

For X direction:

$$\frac{\partial U}{\partial t}+U\frac{\partial U}{\partial x}+V\frac{\partial U}{\partial y}+W\frac{\partial U}{\partial z}=-\frac{1}{\rho}\frac{\partial P}{\partial x}+\frac{\partial}{\partial x}\left(2\mu_e\frac{\partial U}{\partial x}\right)+\frac{\partial}{\partial y}\left(\mu_e\left(\frac{\partial U}{\partial y}+\frac{\partial V}{\partial x}\right)\right)+\frac{\partial}{\partial z}\left(\mu_e\left(\frac{\partial U}{\partial z}+\frac{\partial W}{\partial x}\right)\right) \quad \ldots (2)$$

For Y direction:

$$\frac{\partial V}{\partial t}+U\frac{\partial V}{\partial x}+V\frac{\partial V}{\partial y}+W\frac{\partial V}{\partial z}=-\frac{1}{\rho}\frac{\partial P}{\partial y}+\frac{\partial}{\partial x}\left(\mu_e\left(\frac{\partial V}{\partial x}+\frac{\partial U}{\partial y}\right)\right)+\frac{\partial}{\partial y}\left(2\mu_e\frac{\partial V}{\partial y}\right)+\frac{\partial}{\partial z}\left(\mu_e\left(\frac{\partial V}{\partial z}+\frac{\partial W}{\partial y}\right)\right)+g \quad \ldots (3)$$

For Z direction:

$$\frac{\partial W}{\partial t}+U\frac{\partial W}{\partial x}+V\frac{\partial W}{\partial y}+W\frac{\partial W}{\partial z}=-\frac{1}{\rho}\frac{\partial P}{\partial z}+\frac{\partial}{\partial x}\left(\mu_e\left(\frac{\partial W}{\partial x}+\frac{\partial U}{\partial z}\right)\right)+\frac{\partial}{\partial y}\left(\mu_e\left(\frac{\partial W}{\partial y}+\frac{\partial V}{\partial z}\right)\right)+\frac{\partial}{\partial z}\left(2\mu_e\frac{\partial W}{\partial z}\right) \quad \ldots (4)$$

where; U,V,W are polymer velocities in x, y, z directions. The spinneret inner walls, in the solution domain, presented as no slip condition.

Assumptions

Steady state conditions

Adiabatic system, (No Heat transfer).

The polymer has constant viscosity and density (incompressible flow)

No slip condition at walls.

Influence or change of N2 pressuring tubeshas been neglected.

For the case under study, the values adopted are; viscosity: Pa.s, density: 1.2 kg/m3, exit velocity: 0.4 m/s, Do/Di:0.6/0.3mm

Figure-3 presents screen shots of the CFD model(s) on CAD/CAM screen and after meshing on CFD software.

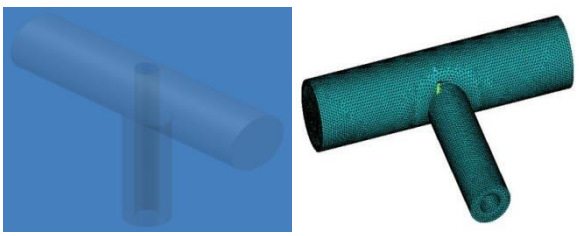

Figure-3. The volume inside which the polymer flows on CAD/CAM and CFD software screens.

The uniformity of exit polymer flow from the new spinneret design is a milestone in success of spinning process. Therefore a CFD study has been performed to ensure the flow uniformity before doing the experimental study.

RESULTS AND DISCUSSIONS

Rheological studies results

The experimental data of different dope compositions including (CA, PS, Plasticizer (Pl), PVP and PEG) have been correlated with viscosity (v) as shown in Figure-4 according to the following correlation noting that

the normalized (n) compositions have been adopted as related to corresponding maximum values:

$$v = 2.8 + 1.5 \times (CA)n + 2.4 \times (PS)n + 4.3 \times (PL)n - 1.8 \times (PVP)n + (PEG)n$$

R=91.5%

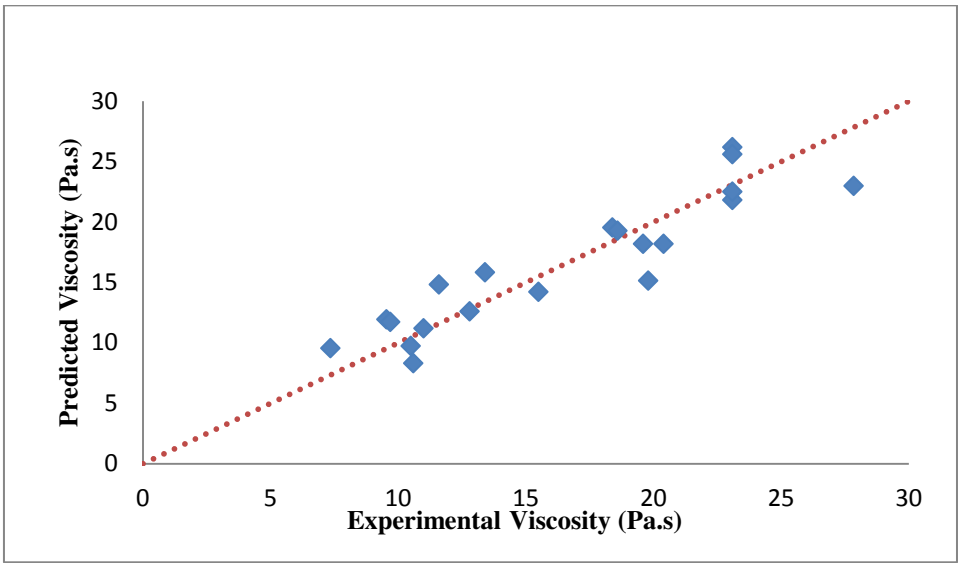

Figure-4. Experimental versus predicted viscosities for different CA dope compositions.

Investigation of Rheological characteristics of the sample dopes (CA1-CA3) in Table-1 indicated variation of viscosities with temperature using different additives (PS/PVP/PEG) as shown in Figure-5.

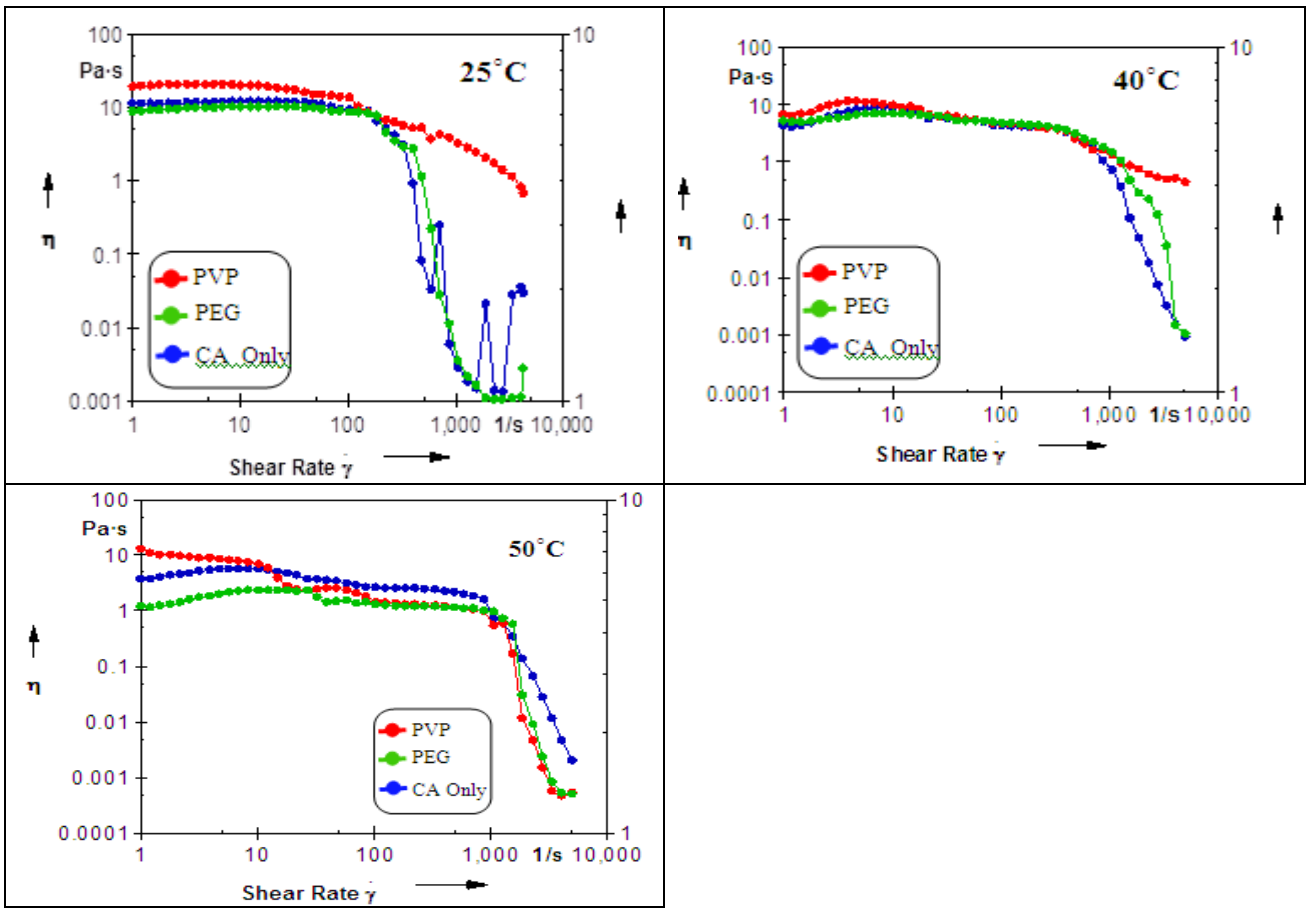

Figure-5. Viscosity dependence of shear rate for dopes with and without additives at (a) 25˚C, (b) 40˚C and (c) 50˚C.

Results indicated minor viscosity changes up to 100s-1 shear rate. At higher shear rate there is a decrease in viscosity up to 1000s-1 shear rate which indicates that shear rate dependent viscosity is manifested from 100s-1 to 1000s-1. Above this shear rate value shear thinning effect is observed. Thus, it may be perceived that the first zone up to 100s-1 is almost Newtonian regime while, the second zone follows a complex shear dependent rheological behavior. Surprisingly, the employed additives (PS/PVP/PEG) did not affect significantly such zone demarcation.

It is apparent that temperature affects the transition point between almost Newtonian to the shear thinning zone. The maximum departure of transition point is manifested by the highest temperature (50°C). The maximum shear stress/ shear rate are manifested by PVP addition.

Shear stress has been also computed to explore the spinneret induced stresses within the spinneret under the prevailing operating conditions on HF fabrication process. Our investigation confirms (data not shown) the prevailing laminar flow regime within the spinneret. Further, the shear rate has been calculated indicating also working in the almost Newtonian regime (up to 100s-1). Such condition will affect the morphological and performance behavior of the fabricated HF which is confirmed by the work of other authors [Yang (2007)].

Design validation of the custom made spinneret

Design configuration of the custom made spinneret has been analyzed using CFD analysis for the polymer flow using the governing equations (1-4). It is indicated that polymer total velocity gradually increases till reaching the fiber casting (production) speed, while the pressure drops by the effect of polymer interlayer and wall friction. Further, increasing spinneret dimensions (inlet/outlet diameters) do not change the polymer behavior but alter the velocity and pressure values. However, the pressure difference increases with themass flow rate due to higher viscous friction. The CFD analysis as depicted in Figure-6 indicates that plug flow occurs just after polymer extrusion from the spinneret orifice.

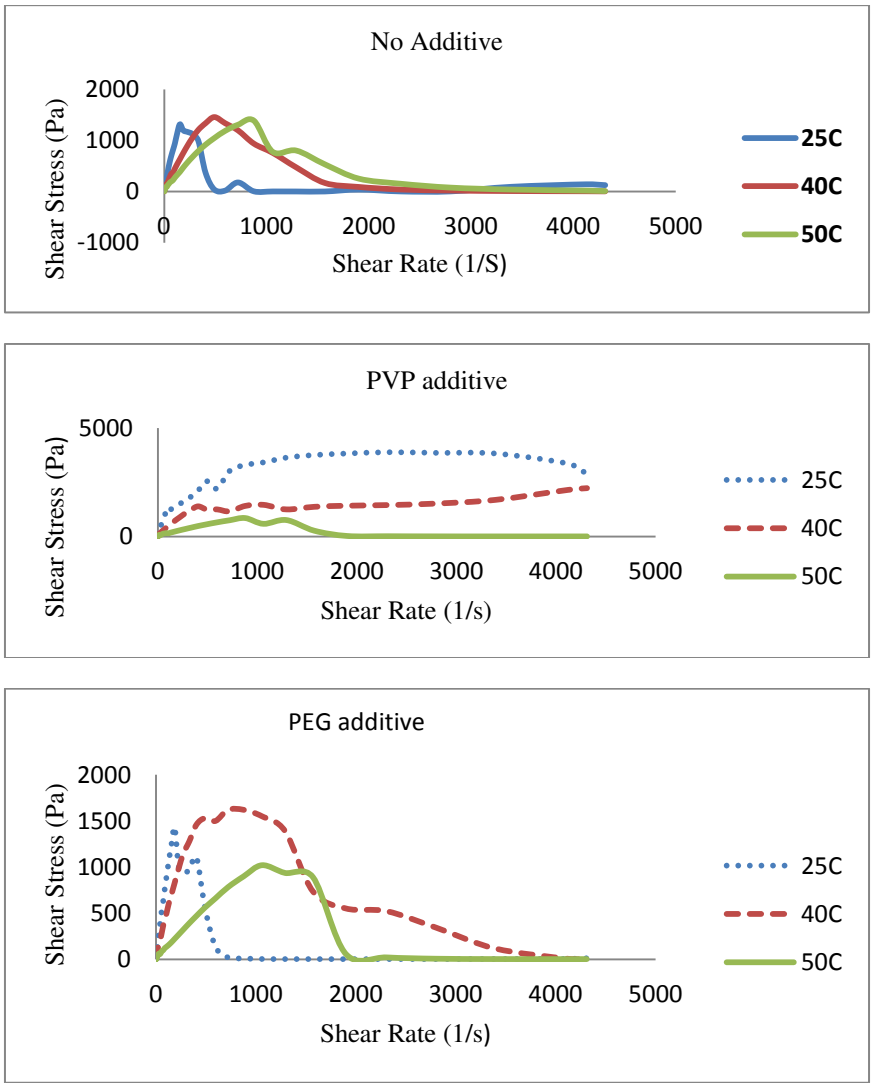

Figure-6. Shear stress dependence on shear rate for dopes (a) without additives, (b) with PVP additive and (c) with PEG additive.

Variations in the velocity distribution and the cross-sectional shape take place mainly in a local region, several tenths of millimetres from the spinneret, and it is a small distance compared with the orifice radius [Yang (2007)] (Figure-7).

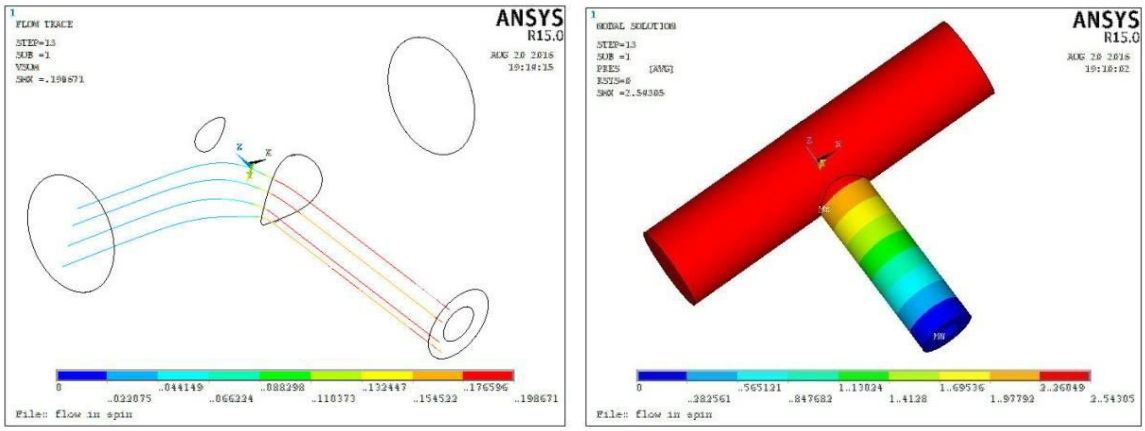

Figure-7. Polymers velocity tracing points, and pressure distribution.

The exit velocity dependence on applied pressure as computed by the CFD is depicted in Figure-8.

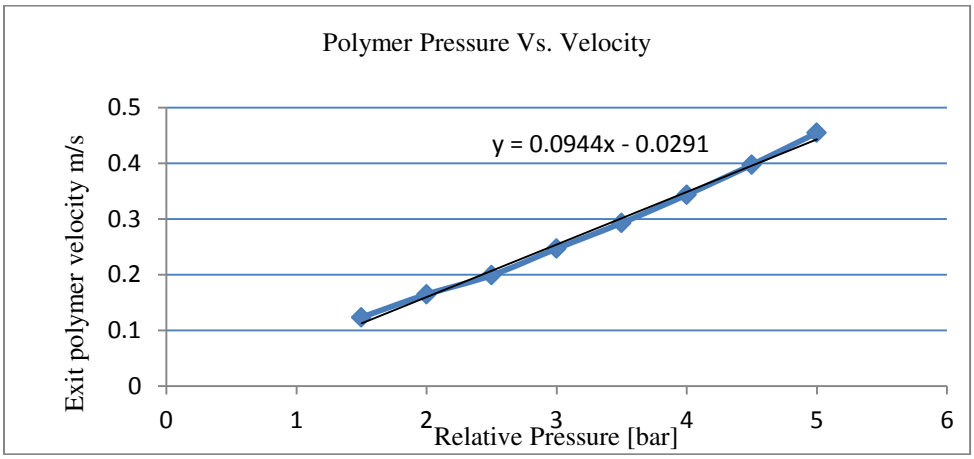

Figure-8. Applied pressure effect on casting (production) speed.

Morphological studies

This section comprises experimental testing of the custom made spinneret using dope blends as presented in Table-1. Further, detailed analysis of the HF morphology have been undertaken for HF samples made from dope blends prepared from both custom made and procured samples.

Testing of the custom made spinneret

Graphical solution of the CFD package confirms the stability of the flows within the dope as bore compartment. Further, design validation has been undertaken using 3 different dopes (CA3, CA4 and CA 8). The SEM images are shown in Figure-9. It is obvious that the HF dimensions cope well with the design objectives. The membrane matrices are well configured with 3 layers inner, middle and outer layer.

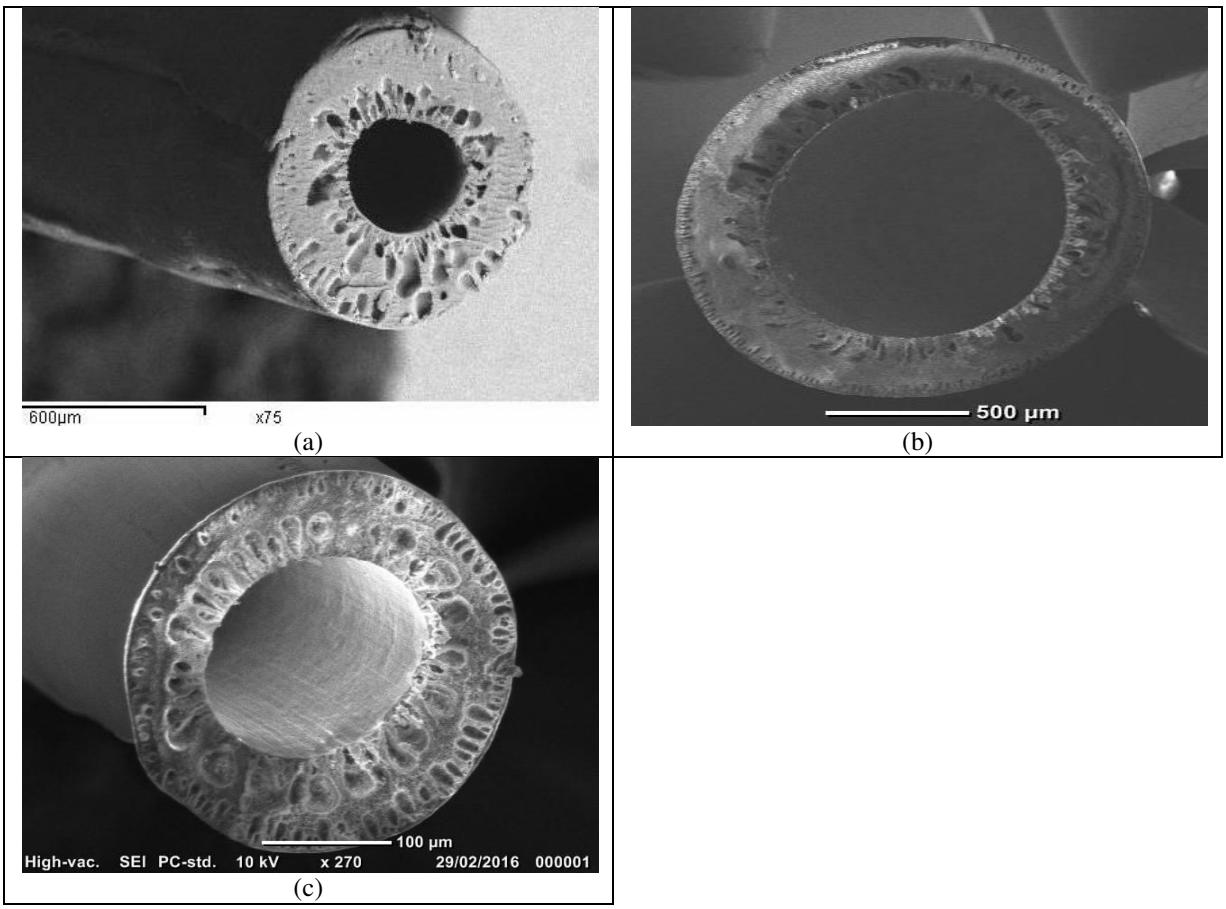

Figure-9. SEM cross-sectional images of some selected CA HF membranes (a) CA3, (b) CA4 and (c) CA8.

Morphological analysis

Samples (CA3, CA4, CA8) present morphological analysis of dope composition comprising (CA: 19%, PEG: 3%, NMP: 78%), CA4 (CA: 22.5%, PS: 4%, NMP: 66.5%, Pl: 5%, PEG: 2%, LiCL:0.7%, ethanol: 1%) and (CA: 20%, PES: 3%, NMP: 68%, PEG: 1%,%, PVP: 3%, Pl:4%, Ethanol: 1).

The SEM images of wall thickness are shown in Figure-10. These figures indicate well structure matrices of outer, middle and inner layers. Data indicates the soundness of the dope composition and operating condition for fabrication of cellulose acetate based HFMs. It also indicates the comparable features of matrices using both customs made and procured spinneret.

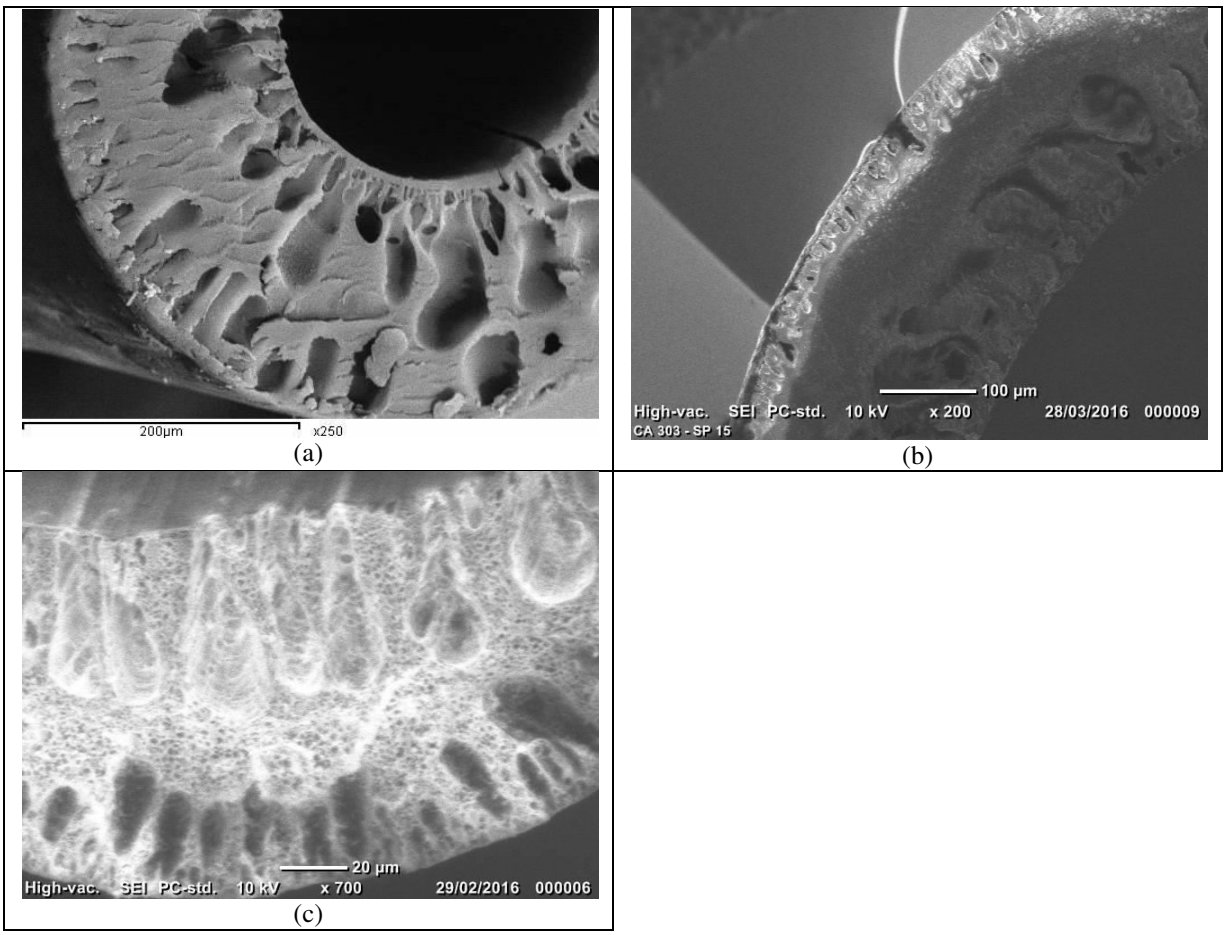

Figure-10. Wall thickness SEM images of some selected CA HF membranes (a) CA3, (b) CA4 and (c) CA8.

AFM Findings

Average roughness (Ra) and root mean square roughness (Rms) are highly connected with fouling tendency as indicated by [Hobbs *et al* (2006)]. Typical AFM image are shown in Figure-11. Roughness data are summarized in Table-3. The obtained relatively low values of roughness indicate that the hollow fibers prepared under the specified conditions would exhibit low fouling properties.

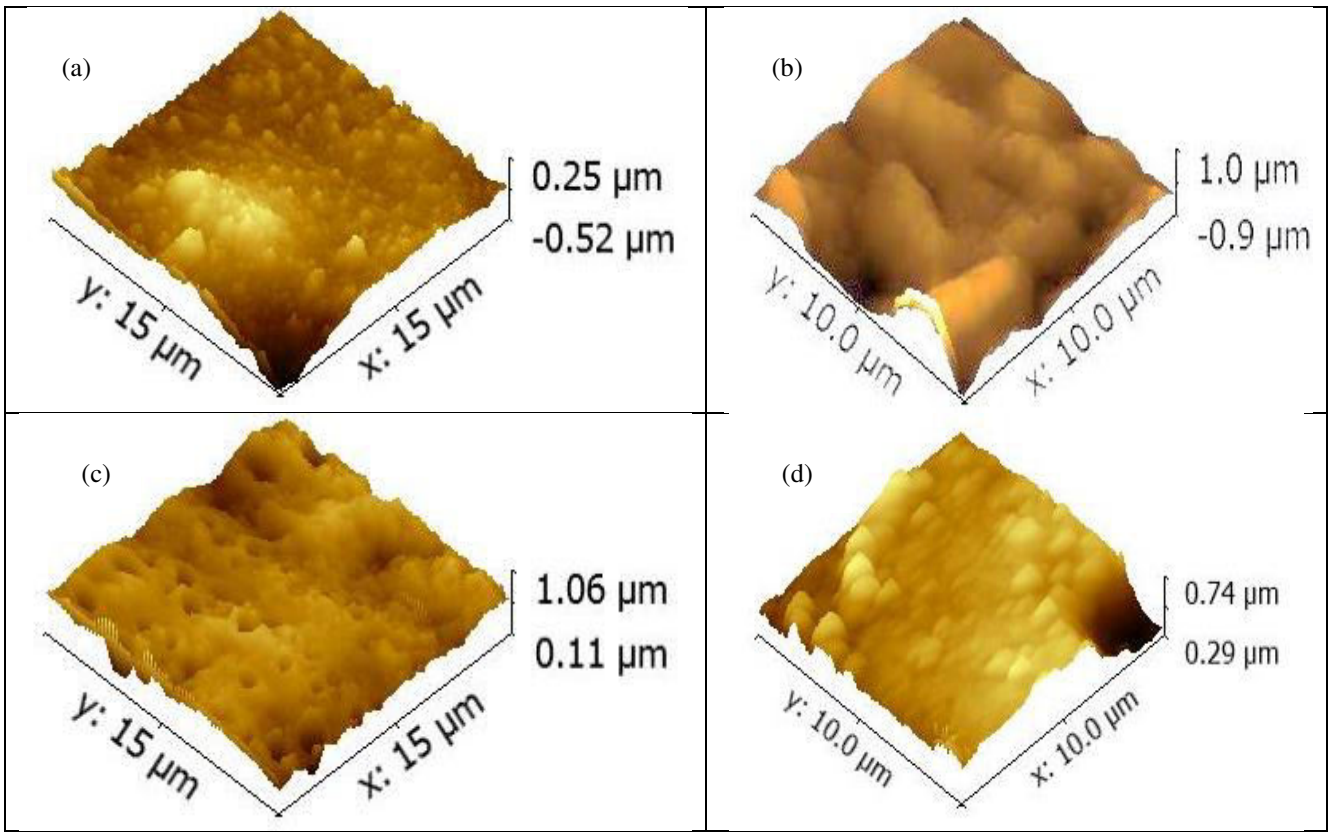

Figure-11. Typical AFM images a) CA4, b) CA5, c) CA 8 and d) PES.

Table-3. AFM results for typical samples.

Sample code	AFM	
	Ra (nm)	**Rms** (nm)
CA 4	68.51	88.24
CA 5	134.87	168.47
CA 8	77.3	102.6
PES	42.5	54.9

Mechanical properties

Mechanical properties have been tested for Break stress, Break strain % and Young's Modulus. Results ranged between 8.0- 9.1 MPa, 36.1-50.0 % and 210-258 MPa for the three parameters respectively. Representative Samples of CA are compared with a typical lPES sample Figure-12. Our results are comparable with the findings of other researchers [Alsalhy *et al*. (2014), Zhu *et al*. (2000)].

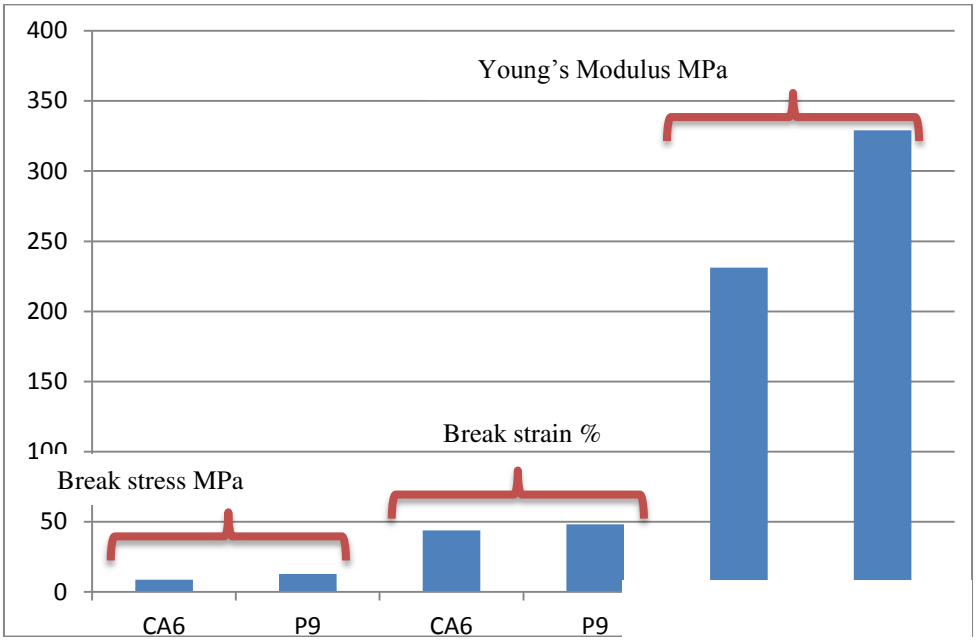

Figure-12. Mechanical properties of selected CA samples as compared with PES sample.

Pure Water Permeability (PWP)

Pure water permeability for selected CA dopes is compared with PES samples of comparable dimension. Water flux results are shown in Figure-13. As observed, flux was relatively high for sample CA 6 although it has been drastically reduced due to pore shrinkage upon being heat treated as reported in previous work [Durbin *et al.* (2013)]. For CA 8 and P9 water flux data are comparable with other reported data for HF MF/UF [Alsalhy *et al.* (2014), Qin *et al.* (2003)].

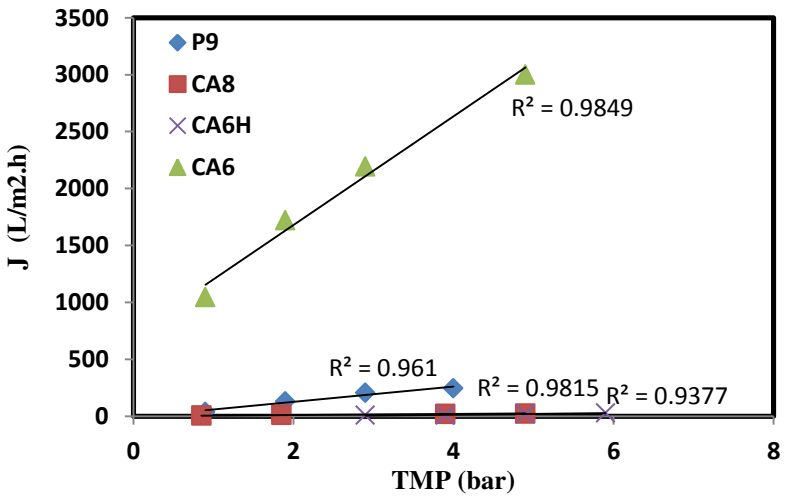

Figure-13. Flux of pure water for typical CA and PES samples.*CA6H is CA6 HT at 80°C for 10 min.

CONCLUSIONS AND RECOMMENDATIONS

CA HF membranes have been fabricated, characterized and tested for water permeations. Custom made spinnerets have been designed and evaluated by CFD and experimentally. Exploration of Rheological aspects has been conducted for selected dope to confirm spinning in the almost Newtonian zone (μ -shear rate pattern).

Morphological (Ra) roughness and mechanical aspects have been investigated and compared with fabricated PES HF membranes. Performance evaluation for CA and PES HS samples indicate adequate permeation rates (MF, UF).

Additional investigations are still needed to develop novel spinning dopes using new CA derivatives and appropriate plasticizers. Endeavors to developed efficient spinnerets should be encouraged to improve fiber characteristics. Costs of chemicals and additives in addition to environmental challenges necessitate interventions to mitigate likely adverse environmental

impacts. Drying processes using non-conventional methods such as MW heating should be incorporated and adopted to continuous process.

Notations

A	Effective membrane area (m2)
CA	Cellulose acetate
CFD	Computation Fluid Dynamics
CTA	Cellulose triacetate
Di	Inside membrane diameter (µm)
DMAc	Dimethylacetamide
Do	Outside membrane diameter (µm)
DT	Drying temperature (oC)
G	Air gap (cm),
HF	Hollow Fiber
HT	Heating temperature (oC)
J	Flux (L/m2.h)
MF	Microfiltration
NMP	N-methyl-2-pyrrolidone
PAN	Polyacrylonitrile
PEG	Polyethylene glycol
PES	Polyethersulfone
PVC	Polyvinyl alcohol
PVDF	Polyvinylidene fluoride
PVP	Polyvinylpyrrolidone
PWP	Pure Water Permeability (L/m2·h)
UF	Ultrafiltration
V	Permeation volume of water (L)
WT	Washing bath temperature (oC)
n	Normalized concentrations
v	Viscosity (Pa.s)

ACKNOWLEDGEMENT

This work has been undertaken through a project entitled "Technological and Engineering Development for Production of Desalination Hollow Fiber Membranes" undertaken by the National Research Centre, Egypt with financial support by Islamic Development Bank, Kuwait Development Bank and Academy of Scientific Research through the Ministry of International Cooperation.

REFERENCES

Alsalhy Q. F., Salih H. A., Simone S., Zablouk M., Drioli E. and Figoli A. 2014. Polyethersulfone (PES) hollow-fiber membranes prepared from various spinning parameters, Desalination. 345:, 21-35.

Antonietti P. F., Fadel N. A. 2011. Verani, M.,Modelling and numerical simulation of the polymeric extrusion process in textile products, Communications in Applied and Industrial Mathematics. 1(2): 1-13.

Aptel P.; Abidine N.; Ivaldi F.; Lafaille J.P.J. 1985. Polysulfone hollow fibers effect of spinning conditions on the ultrafiltration properties, J. Membr. Sci. 22: 199.

Baker R. W. 2004. Membrane Technology and Applications. 2nd Ed, John Wiley & Sons, Chichester.

Cao C, Chung TS, Chen SB, Dong Z.J. 2004. The study of elongation and shear rates in spinning process and its effect on gas separation performance of poly(ethersulfone) (PES) hollow fiber membranes, Chem Eng Sci. 59: 1053-1062.

Chen G-E. Li J-F., Han L-F., Xu Z-L., Yu Li-Y. 2010. Preparation of Micro-porous Polyethersulfone Hollow Fibre Membranes Using Non-solvent Vapor-induced Phase Separation, Iranian Polymer Journal. 19(11): 863-873.

Chou W. L. & Yang M. C. 2005. Effect of coagulant temperature and composition on surface morphology and mass transfer properties of cellulose acetate hollow fiber membranes, Polymers for Advanced Technologies. 16(7): 524-532.

Chou W-L, Yu D-G., Yang M-C. 2007. Effect of molecular weight and concentration of PEG additives on morphology and permeation performance of cellulose acetate hollow fibers, Separation and Purification Technology. 57(2):209-219.

Chung T.S., Xu, Z-L, Lin, W. 1999. Fundamental Understanding of the Effect of Air-Gap Distance on the Fabrication of Hollow Fiber Membranes, J. Appl. Polym. Sci. 72(3): 379-395 .

Chung T.S. Qin J.J., Gu J. 2000. Effect of shear rate within the spinneret on morphology, separation performance and mechanical properties of ultra-filtration polyethersulfone hollow fiber membranes, Chem. Eng. Sci. 55: 1077-1091.

Chung T.S., Qin J.J., Huan A., Toh K.C. 2002. Visualization of the effect of die shear rate on the outer surface morphology of ultrafiltration membranes by AFM, J. Membr. Sci. 196: 251-266.

Durbin C., Hausman R., Escobar I.C. 2013. An investigation of polymer dope and heating effects on hollow fiber membranes, Desalination and Water Treatment. 51: 6970-6977.

Ehsan S., Toraj. M. 2009. Cellulose acetate (CA)/polyvinylpyrrolidone (PVP) blend asymmetric membranes: Preparation, morphology and performance Desalination. 249: 850-854.

Feng C.Y., Khulbe K.C., Matsuura T., Ismail A.F. 2013. Recent progresses in polymeric hollow fiber membrane preparation, characterization and applications, Separation and Purification Technology. 111: 43-71.

Hao J-H., Dai H., Yang P., Wei J., Wang Z. 1996. Cellulose acetate hollow fiber performance for ultra low pressure RO, Desalination. 107: 217.

Hobbs C., Hong S., Taylor J. 2006. Effect of surface roughness on fouling of RO and NF membranes during filtration of a high organic surficial groundwater. Journal of Water Supply: Research and Technology, AQUA. 55(7): 8.

Idris A., Ismail, A.f., Noordin M.Y. and Shilton S. J. S. J. 2002. Optimization of Cellulose acetate hollow fiber reverse osmosis membrane production using Taguchi method, J. Membr. Sci. 205: 223-237.

Idris A, Ismail A.F., Gordeyev S.A., Shilton S. J. 2003. Rheology assessment of cellulose acetate spinning solution and its influence on reverse osmosis hollow fibre membrane performance, Polymer Testing. 22: 319-325.

Idris A., Noordin M. Y., Ismail A. F, Shilton S. J. 2002. Study of shear rate influence on the performance of cellulose acetate reverse osmosis hollow fibre membranes, J. Membr. Sci, 202: 205-215.

Khayet M. 2003. The effect of air gap length on the internal and external morphology of hollow fiber membranes. Chem. Eng. Sci. 58: 3091-3104.

Kim J.Y., Lee H.K. Kim S.C. 1999. Surface structure and phase separation mechanism of polysulfone membrane by atomic force microscopy, J. Membr. Sci. 163: 159-166.

Miyano T., Matsuura T., Sourirajan S. 1993. Effect of polyvinyl pyrrolidone additive on the pore size and pore size distribution of polyethersulfone (Victrex) membranes, Chem. Eng. Commun. 119: 23.

Nunes S.P., Peinemann K.V. 2006. Membrane Technology in the Chemical. Industry, Wiley-VCH, 2nd ed.

Orofino T.A. 1977. Technology of hollow fiber reverse osmosis membrane systems, in: Sourirajan (Ed.) Reverse osmosis and synthetic membranes, National Research Council Canada, Ottawa. pp. 313-340.

Qin J and Chung T. S. 1999. Effect of dope flow rate on the morphology, separation performance, thermal and mechanical properties of ultrafiltration hollow fibre membranes, J. Membr. Sci, 157: 35-51.

Qin J.J., Li Y., Lee L.S., Lee H. 2003. Cellulose acetate hollow fiber ultrafiltration membranes made from CA/PVP/NMP/Water, J. Membr. Sci. 218: 173.

Qin J-J., Oo, M.H., Cao Y-M., Lee L-S. 2005a. Development of a LCST membrane forming system for cellulose acetate ultrafiltration hollow fiber, Separation and Purification technology. 42(3): 291-295.

Qin J.J, Li Y. 2005b. Effect of hypochlorite concentration on properties of post-treated outer skin ultrafiltration membranes spun from CA/PVP blends, J. Appl. Polym. Sci. 97: 227-231.

Ren J.Z. and Wang R. 2008. Preparation of polymeric membranes. in Membrane and Desalination Technologies, Handbook of Environmental Engineering, Volume 13, Lawrence K. Wang, J. Paul Chen, Yung-Tse Hung and Nazih K. Shammas (eds). 47-100.

Shieh J. J. and Chung T. S, 1998. Effect of liquid-liquid demixing on the membrane morphology, gas permeation, thermal and mechanical properties of cellulose acetate hollow fibres, J. Membr. Sci. 140, 67-79.

Stamatialis D.F., Dias, C.R. Pinho, M.N. 1999. Atomic force microscopy of dense and asymmetric cellulose-based membranes, J. Membr. Sci. 160, 235-242.

Tung KL, Li YL, Hu CC, Chen YS. 2012. Power law polymer solution flow in a converging annular spinneret: Analytical approximation and numerical computation, AIChE Journal. 58(1): 122-131.

Wienk I.M., Boomgaard Th. V.D., Smolders C.A 1994. The formation of nodular structures in the top layer of ultrafiltration membranes, J. Appl. Polym. Sci. 53: 1011-1023.

Xu Z.L., Qusay F.A. 2004. Polyethersulfone (PES) hollow fiber ultrafiltration membranes prepared by PES/non-solvent/NMP solution, J. Membr. Sci. 233: 101-111.

Yang Su. 2007. Theoretical studies of hollow fiber spinning, PhD thesis, The University of Toledo, MI, USA.

Zhang L. *et al*. 2013. Pressure Distribution on Spinning Spinnerets, Thermal Science. 17(5): 1533-1537.

Zhang Y.P., Shao H.L., Hu X.C. 2002. Atomic force microscopy of cellulose membranes prepared from the N-methylmorpholine-N-oxide/water solvent system, J. Appl. Polym. Sci. 86: 3389-3395.

Zhu G.-H., Chung T.-S., Loh K.-C. 2000. Activated carbon-filled cellulose acetate hollow-fiber membrane for cell immobilization and phenol degradation, J. Appl. Polym. Sci. 76: 695.